Journal of Applied Geophysics 70 (2010) 255–265

Contents lists available at ScienceDirect

Journal of Applied Geophysics

journal homepage: www.elsevier.com/locate/jappgeo

The use of non-conventional CPTe data in determination of 3-D electrical resistivity distribution

Zsuzsanna Nyári [a], Ali Ismet Kanlı [b,*], János Stickel [c], Axel Tillmann [d]

[a] Eötvös Lorand Geophysical Institute of Hungary, P.O. Box 35, H-1440 Budapest, Hungary
[b] Istanbul University, Engineering Faculty, Department of Geophysical Engineering, 34320, Avcilar, Istanbul, Turkey
[c] Elgoscar 2000 Ltd., Budapest, Hungary
[d] Institute of Dynamics and Chemistry of the Geosphere, ICG-IV, Agrosphere, Forschungszentrum Jülich GmbH, 52425 Jülich, Germany

ARTICLE INFO

Article history:
Received 30 May 2009
Accepted 22 January 2010

Keywords:
CPTe resistivity
Well-log interpretation
ERT
3D resistivity distribution
Contamination

ABSTRACT

The spatial distribution of the electrical resistivity data provides useful information for investigating and modeling the fluid transport processes. 3D electrical resistivity distribution provides information about water flow and changes in electrical resistivity of the pore fluid.

Therefore, to assist in understanding and modeling of the fluid transport process, 3D spatial distribution of the electrical resistivity data with the corresponded 3D geological section were mapped and interpreted in the test site located in western Germany. A process of deriving electrical resistivity values from the mechanical and radioactive parameters of cone penetration tests (CPT) and geological information of boreholes was presented. A reliable method which gives accurate resistivity values in cases of near surface sediments was introduced. Then a field test was executed where the calculated resistivity values were compared with the measured CPTe resistivity data. The CPTe (cone penetration test with electrical extension) data were also used in correlating to the ERT (electrical resistivity tomography) data. Consequently, obtained dense CPT surveys give us the possibility to determine a high resolution resistivity distribution of the investigated area.

1. Introduction

One of the most critical encountered tasks to remediation of polluted environment is determining the 3-D spatial distribution of contaminants which stimulate us to provide accurately modeled subsurface. Although there are several conventional methods for modeling the subsurface, to understand the hydrogeological process and spatial distribution of contamination, these methods can be gathered under two main branches that are invasive (e.g. invasive, semi-invasive, less-invasive) and non-invasive techniques. Classical borehole techniques, SPT and CPT are among the invasive or less-invasive techniques whereas electrical and electromagnetic based ERT and GPR, most widely used techniques in imaging the subsurface in the last decade (Nyari and Kanlı, 2007), are called as non-invasive geophysical methods.

Ground penetrating radar data have been used to provide images of dielectric permittivity contrasts, which are used to deduce variations in subsurface geology. Additionally, recent developments in processing, inversion and estimation approaches illustrate that GPR methods can be very useful for obtaining quantitative information about subsurface properties (Lambot et al., 2008). On the other hand, ERT data which can be inverted to determine the subsurface electrical conductivity structure are increasingly being used to help the development of subsurface models. Data can be used to derive the existence of contaminants and to obtain flow directions of contaminants due to their electrical conductivity differences from the background environment (Pidlisecky et al., 2006; Daily and Ramirez, 1995; LaBrecque and Yang, 2001; Versteeg et al., 2000; Kemna et al., 2002; Slater et al., 2002; Singha and Gorelick, 2005).

In some cases, boreholes are considered unfavorable in contaminated sites due to high costs, time consuming of field duration, some risks the exposure of workers to contaminants and drillings can cause mobilizing of the contaminants by creating new pathways in the subsurface. To overcome these problems, Pidlisecky et al. (2006) have developed a cone-based electrical resistivity tomography system.

On the other hand, precise understanding of 3-D contamination distribution in the subsurface still needs the combination of sensitive less-invasive borehole geophysical technology with the non-invasive surface geophysical methods.

Numerical modeling methods are more frequently used to describe the behavior of pollutants in soils and groundwater, and to perform risk assessment of potentially hazardous substances. However, validation of the models requires precise knowledge of the spatial and temporal variation of fluid transport properties (Szücs and Madarasz, 2006).

The electrical resistivity of porous media is concerned to the saturation of the pore space with fluid via various empirical formulas. The 3D

* Corresponding author
E-mail address: kanli@istanbul.edu.tr (A.I. Kanlı).

0926-9851/$ – see front matter © 2010 Elsevier B.V. All rights reserved.
doi:10.1016/j.jappgeo.2010.01.008

distribution of electrical resistivity provides information about water flow and changes in the electrical resistivity of the pore fluid. Owing to the determination of high resolution spatial resistivity distribution in near surface sediments is not an easy task with conventional surface and/or invasive measurement methods. Dense in situ measurement methods such as electrical resistivity tomography (ERT) or cone penetration technology (CPT) are successfully used for this purpose.

The cone penetration test (CPT) is accepted as fast and proper technology for in situ measurements in shallow unconsolidated sediments due to its capacity for resolving the structure of the subsoil in detail. Additionally, it is able to obtain various physical parameters during soil penetration. The method is suitable for investigating loose, near surface sediments e.g. clay, sand or gravel. A hydraulic device, anchored to the ground, pushes a string of pipes into the subsurface. The crossed geological structures are hardly deformed because of the small diameter which is 44 mm. Contrary to the traditional drilling methods, the measured CPT data can be considered almost as being in situ. The penetration depth reaches to the top of the bedrock, or to the granular sediments which have good technical conditions in 20–30 m. depths. The details of the CPT technology are given by Lunne et al. (1997).

A spatially dense sampled CPT survey was organized in order to investigate the stratigraphy as well as the spatial variability of the soil properties with grain size distribution and hydraulic conductivity at the test site of Krauthausen in Germany in 2003 and 2004 (Tillmann et al., 2005). The purpose of the research was to provide detailed petrophysical and stratigraphical parameters for further numeric fluid transport models. An investigation depth of up to 16 m was reached. The mechanical cone resistance, the natural gamma activity, the bulk density, and the volumetric water content were measured at about 10000 sampling points. Additionally the electrical resistivity was measured at about 2000 sampling points. It was proved that CPT method is a suitable tool for giving detailed and reliable information about the aquifer's physical parameters (Tillmann et al., 2005). Parallel to previous studies at the test site of Krauthausen and by using the huge data set, we try to present a process of deriving electrical resistivity values from the mechanical and radioactive parameters of cone penetration tests (CPT) and geological information of boreholes. For this aim, we investigated a suitable method to obtain reliable resistivity values in cases of near surface sediments. Then a field test was executed where the calculated values were compared with the measured CPTe resistivity data called as penetration tests extended with electrical resistivity measurements. In our special version of CPT measurements, we used both the CPTe data and nuclear data. Close spaced (10 cm) measurements of various physical parameters depending on the transverse layers are carried out either during the pushing process with sensors placed on the tip of the pipe or after the pushing, using probes moved inside the pipes. During the pushing process, hydraulic, cone pressure and eventually electrical resistivity values were recorded. Inside the pipes radioactive parameters were also measured.

For the special near surface characteristics of the method, the conventional data interpretation techniques of well loggings can be applied with some reviewing and modifications. Therefore a suitable method was needed to determine 3D spatial distribution of the electrical resistivity in the test area. The input data of the electrical resistivity calculation were the petrophysical parameters defined from the dense CPT parameters. The output resistivity values were validated through comparing the calculated and measured values and also compared with the ERT data crossed through the same profile. After successful validation, a high resolution 3D electrical resistivity distribution of the investigated area of Krauthausen test site is presented.

2. Petrophysical parameters from CPT data

By executing the cone penetration test with the method described by Fejes and Jósa (1990), five quantities are recorded: Cone resistance (MPa), natural gamma activity (counts per minute), gamma-gamma and neutron activity. Optionally, when an additional probe is assembled to the system, the electrical resistivity can be recorded.

In general, nuclear measurements are not directly used in the interpretations but they are used to determine some physical characteristics by calibrating the radioactive probes against the reference materials. The recorded data of gamma–gamma and the neutron activity can be converted to bulk density and water content whereas the measured natural gamma activity is related to the clay content of the soil. According to Fejes et al. (1997), natural gamma activity can be used in grouping the soils as clay which is non-permeable (activity ≥1700 counts/min, signature is black), silt which is semi-permeable (activity is 800–1700 counts/min, signature is dark-gray) and gravel/sand which are permeable (activity <800 counts/min, signatures are light-gray).

3. Determination of electrical resistivity

Here, we classified and analyzed the determination of electrical resistivity values by empirical laws and models. Three important methods are given as follows;

3.1. Archie model

Archie's law (1942) describes the connection of stratigraphical parameters and electrical resistivity ($R_t^{(T)}$) for porous media composed of non-conducting matrix minerals and saturated with water as given in Eq. (1).

$$R_t^{(T)} = \frac{R_w}{\Phi^m S_w^n} \tag{1}$$

In the equation, Φ is porosity, m is cementation exponent, n is saturation exponent (taken as 2 in the study), R_w is the resistivity of pore water and S_w is expressed as water saturation. According to this empirical law, electrical conduction is assumed not to be present within the rock grains or in fluids other than water. The parameters of Eq. (1) can be easily determined from CPT parameters (Table 1).

Comparison between the measured CPTe resistivity data and the calculated resistivity values of Archie's method from the CPT log of the borehole JT32A is presented in Fig. 1. A bar chart follows the normalized deviation of the two values. Simply the deviation is calculated by the given equation;

$$\text{Deviation} = \sqrt{\frac{(\text{Measured.Data} - \text{Calculated.Data})^2}{(\text{Measured.Data})^2}}. \tag{2}$$

The depth function of the natural gamma activity is also presented. This parameter is directly connected to the clay content of the sediment. After a calibration process the sand and clay boundaries are defined. These boundaries are marked with dashed lines in Fig. 1. The two resistivity curves fit each other where the gamma intensity stays below the sand line. As soon as it gets over the sand line the deviation of the model and true resistivities become significant.

In general, clay bearing formations are recorded as less resistive in contrast to the dry clay which is highly resistive, because they contain

Table 1
Parameters and their origins calculated from CPT data.

Parameters	Origin
Φ	Calculated from gamma and neutron porosity logs
m	Result of optimization process by using the values of mechanical (cone) resistance log
R_w	Depth function measured in monitoring wells

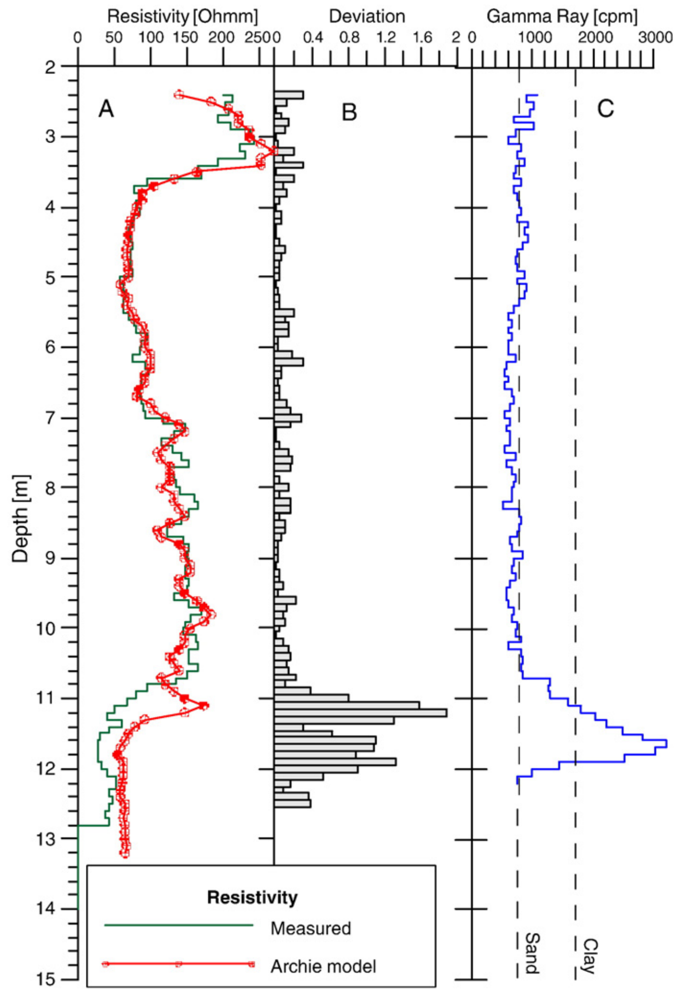

Fig. 1. A) Comparison of CPTe record and resistivity values calculated from Archie's method. B) Deviation plot of CPTe and Archie's method data. C) Natural gamma-ray activity.

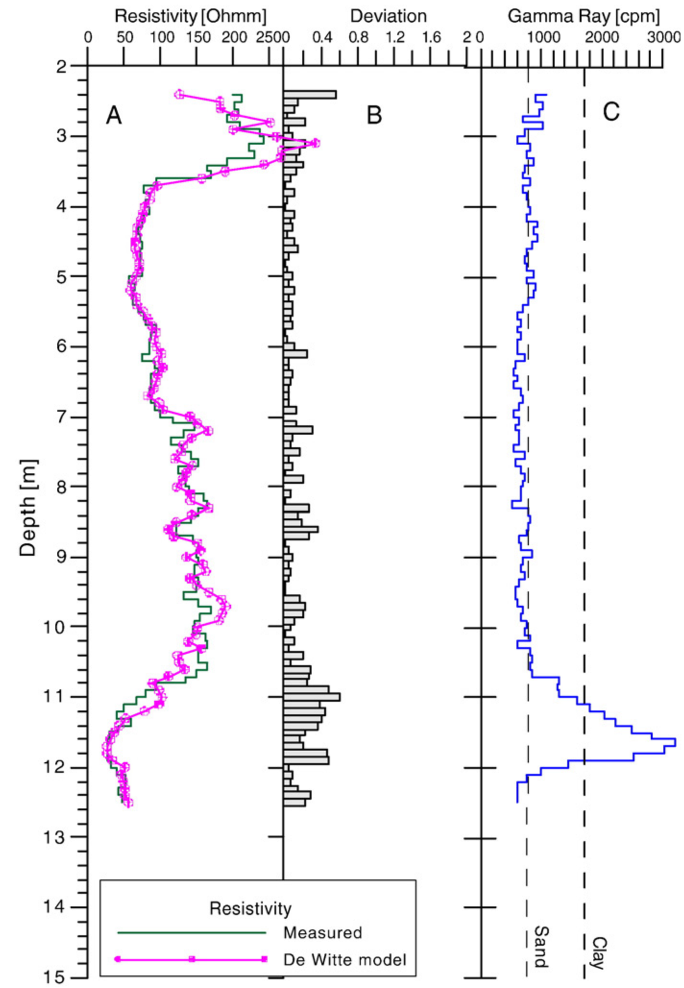

Fig. 2. A) Comparison of CPTe record and resistivity values calculated from Archie's method. B) Deviation plot of CPTe and Archie's method data. C) Natural gamma-ray activity.

several air filled fractures. Clay content is only one of the causes of resistivity but it also highly depends on the water content and consequently it is related to the grain size. At the first meters of the logs, there is a very fine and wet sand which causes the high conductivity, while there is the low resistivity depending on the high clay content at 10.5–12 m in depth.

It is well known that Archie's model disregards the conductivity effect of the layer's clay content; therefore, it is not valid for sediments containing a significant percentage of clay. Fig. 1 demonstrates that the limit of Archie's model is valid in where the sand boundary of natural gamma activity presence in case of near surface sediments.

3.2. Dual water models

Waxman and Smits (1968) introduced a method that corrects Archie's law with the conductivity caused by the clay's structure and cation exchange capacity. The effect of clay is represented by the cation concentration and the average counterion mobility in the corrected formula. Devarajan et al. (2006) studied the application possibilities of Waxman-Smits' and other dual water models in describing the connection of petrophysical parameters and electrical resistivity. The dual water models seem sufficient for porous media but the quantities that are required for resistivity calculations cannot be reliably derived from CPT parameters. Therefore in our calculations we neglected the dual water models.

3.3. De Witte model

De Witte (1957) constructed a model describing the function of electrical resistivity $R_t^{(T)}$ in porous rocks with significant clay content in cases of unsaturated (Eq. (3)) and saturated (Eq. (4)) media.

$$R_t^{(T)} = \frac{1}{(\phi + V_{cl})^m} \frac{1}{\frac{V_{cl}}{\phi + V_{cl}} \frac{1}{R_{cl}} + \frac{\phi}{\phi + V_{cl}} \frac{1}{R_w}} \tag{3}$$

$$R_t^{(T)} = \frac{1}{(\phi + V_{cl})^m} \left(\frac{\phi + V_{cl}}{\phi S_w + V_{cl}} \right)^2 \frac{1}{\frac{V_{cl}}{\phi S_w + V_{cl}} \frac{1}{R_{cl}} + \frac{\phi S_w}{\phi S_w + V_{cl}} \frac{1}{R_w}}. \tag{4}$$

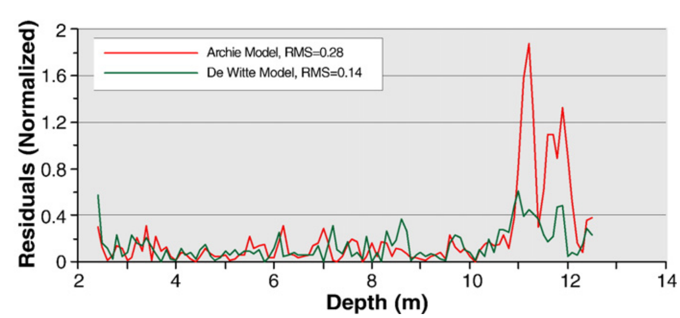

Fig. 3. Normalized residuals of measured and calculated resistivities of two models at push-points JT32A.

Fig. 4. The test area with monitoring wells.

In the equations given above Eqs. (3) and (4), R_{cl}, V_{cl}, Φ, m, R_w and S_w denote clay resistivity, clay volumic fraction of the medium, porosity, cementation factor, resistivity of the pore water, and the water saturation respectively. All these parameters can be derived directly or indirectly from CPT parameters as given at the description of Archie's method. The clay resistivity (R_{cl}) is defined after an optimization process.

Resistivity calculations by using the De Witte model for saturated zone is presented in Fig. 2. In contrary to the Archie's model in given Fig. 1, the conductive effect of the clay intercalation at the depth of 10.5–12 m appeared with the decrease of both measured and calculated resistivity values. The deviation of the two resistivity curves stayed below 0.4 along the whole depth range. Fig. 2 proves that the De Witte model is sufficient for describing the resistivity distribution of porous sediments even with the existence of significant clay content. Consequently, using error calculations and the normalized residuals of measured and calculated resistivities of two models it was proved that because of the conductivity of the layers with high clay content, De Witte's model is suitable for the investigated geological structure more than the commonly used Archie's one (Fig. 3).

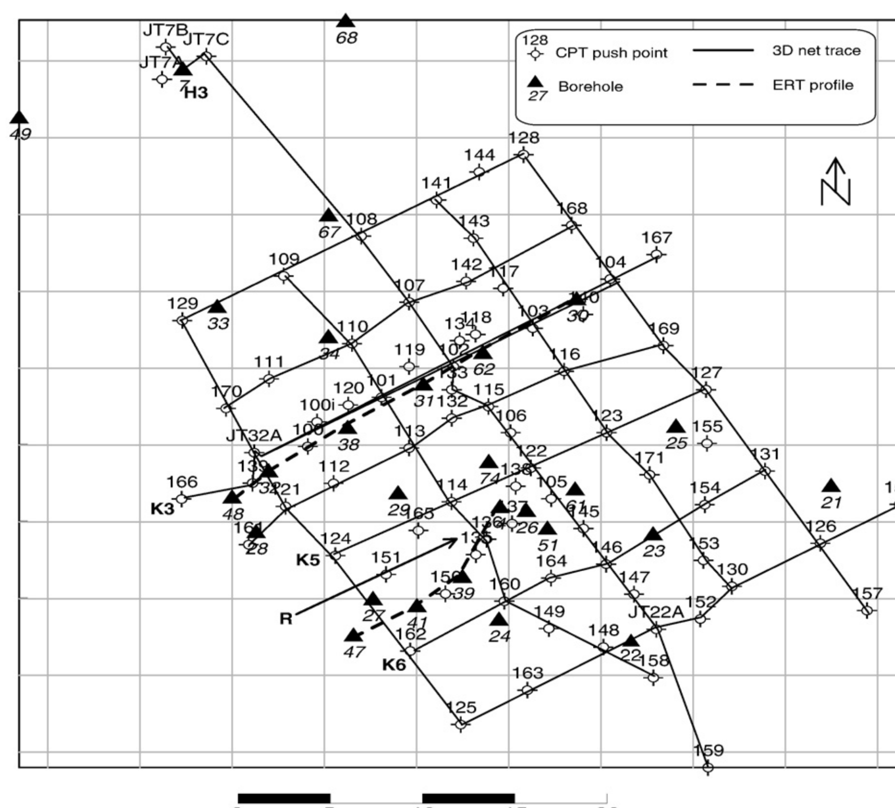

Fig. 5. Location map of CPT and CPTe survey.

4. Test area

The determination method of 3D resistivity distribution from CPT petrophysical parameters was tested on the certificated test area of Research Centre Jülich (Fig. 4). The test site is located in the Lower Rhine Embayment in Western Germany and has an extension of 200 × 70 m. The test area was first set up in 1993 by the Research Centre Jülich to research and execute some experiments on water flow and solute transport processes. Thereafter, several researchers used that test site for various purpose and studies (e.g. Döring, 1997; Vereecken et al., 1999, 2000Kemna et al., 2002; Englert, 2003; Hördt et al., 2007; Tillmann et al., 2008; Li et al., 2008).

The well-known test area was chosen by the researchers due to its knowledge of the hydrogeological situation, detailed information at field scale, the possibility to conduct additional field experiment at the test site, the presence of different stack holders, contains several protection areas designed to safeguard groundwater quality and the presence of pesticides in the groundwater.

The geological profile of the area was defined after 73 boreholes, although only four of them reached the depth of 15–20 m. The aquifer material consists mainly of gravelly and sandy sediments deposited by the braided river system of the Rur. The clay and silt content of the aquifer sediments vary between 0.5% and 7.5% and the mean total porosity is 26 ± 7%. The local base of the aquifer in a depth of 11 to 13 m consists of intermitting thin layers of clay and silt.

In order to ensure sufficient monitoring of the spatial and temporal distribution of the tracer substances as well as to obtain representative sediment materials for aquifer characterization, 68 observation wells with a diameter of 50 mm were installed. Several tracer tests were conceived (e.g. Vereecken et al., 2000) and evaluated using stochastic

Fig. 6. Combined probe for mechanical resistance and electrical resistivity logs (left) and combined probe for natural gamma and gamma gamma logs (right).

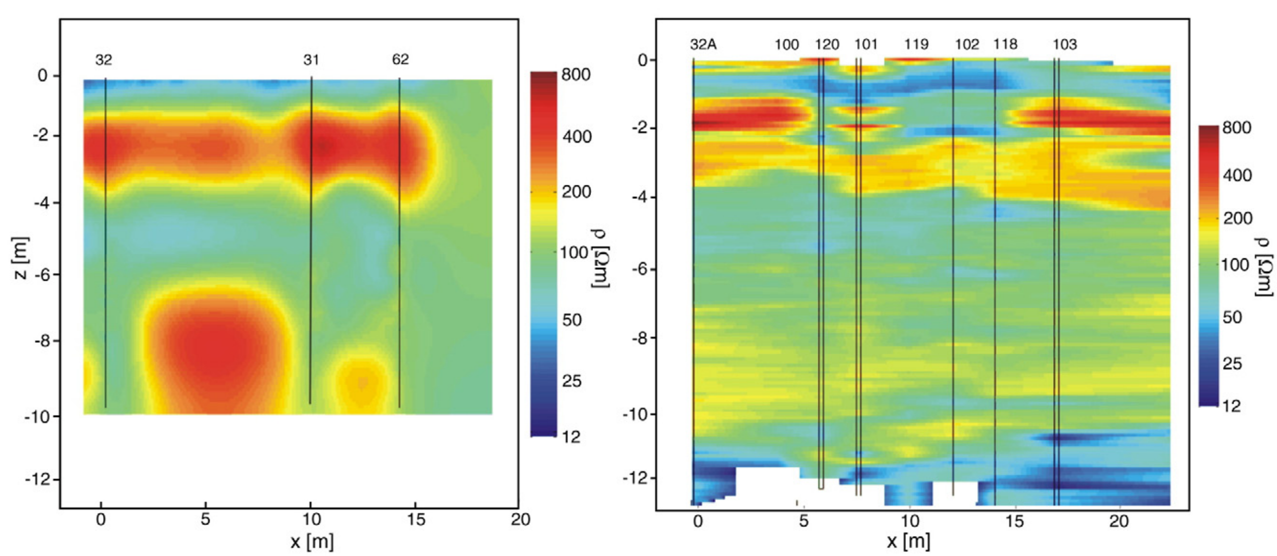

Fig. 7. Resistivity sections of ERT (left) and CPTe (right) measurements. Both measurements are performed at the same profile K3. The ERT measurements were taken in the boreholes whereas the CPTe measurements were taken in push-points given in the location map in Fig. 5.

transport theory based on breakthrough curves of the tracer (Vanderborght and Vereecken, 2002). Electrical resistivity tomography (ERT) was used during the last tracer test (Kemna et al., 2002) for an imaging of solute concentrations, and thus tracer migration, at high spatial resolution. The heterogeneous distribution of physical soil properties required for transport modeling in an aquifer was detected by CPTe method in 2003 and 2004 (Tillmann et al., 2005). Estimation of grain size distribution and hydraulic conductivity with CPT method were executed by Tillmann et al. (2008).

5. Field study

In order to investigate the small-scale heterogeneity of hydraulic conductivity due to different soil parameters a CPT and CPTe survey with 78 push points was performed in a central area of 30x20 m of the test site in 2003 and 2004. In order to provide high horizontal resolution of the measured parameters to achieve a good estimation of the small scale variability and determination of correlation length the push points were placed unusually close to each other; the horizontal sampling interval was in the range of 1.5 m to 3 m. The push points, form a dense net, are placed next to boreholes and along measured or planned ERT profiles (Fig. 5). Three drillings were sampled completely (numbers 7, 22 and 32) within the CPT survey area. The other drillings were sampled only at several depths or not sampled at all. Therefore the geological structure is not reconstructed in detail except for a simplified stratigraphic model.

Because of the geological conditions, electrical resistivity could be registered only at 17 points during the survey. The CPT and CPTe measurements were performed down to 13.5 m depth average and 16 m depth maximum. The vertical sampling interval was 10 cm with the push velocity of about 1 cm/s. During the pushing procedure, the mechanic cone resistance (cr-MPa) and the electrical resistivity (ρ-Ω m) are measured. The pressure sensor is placed on the tip of the measuring head, and there is a 3 + 1 electrode system inserted on the measuring head. After the pushing process a passive natural gamma probe and two radioactive probes (gamma gamma and neutron log) are moved inside

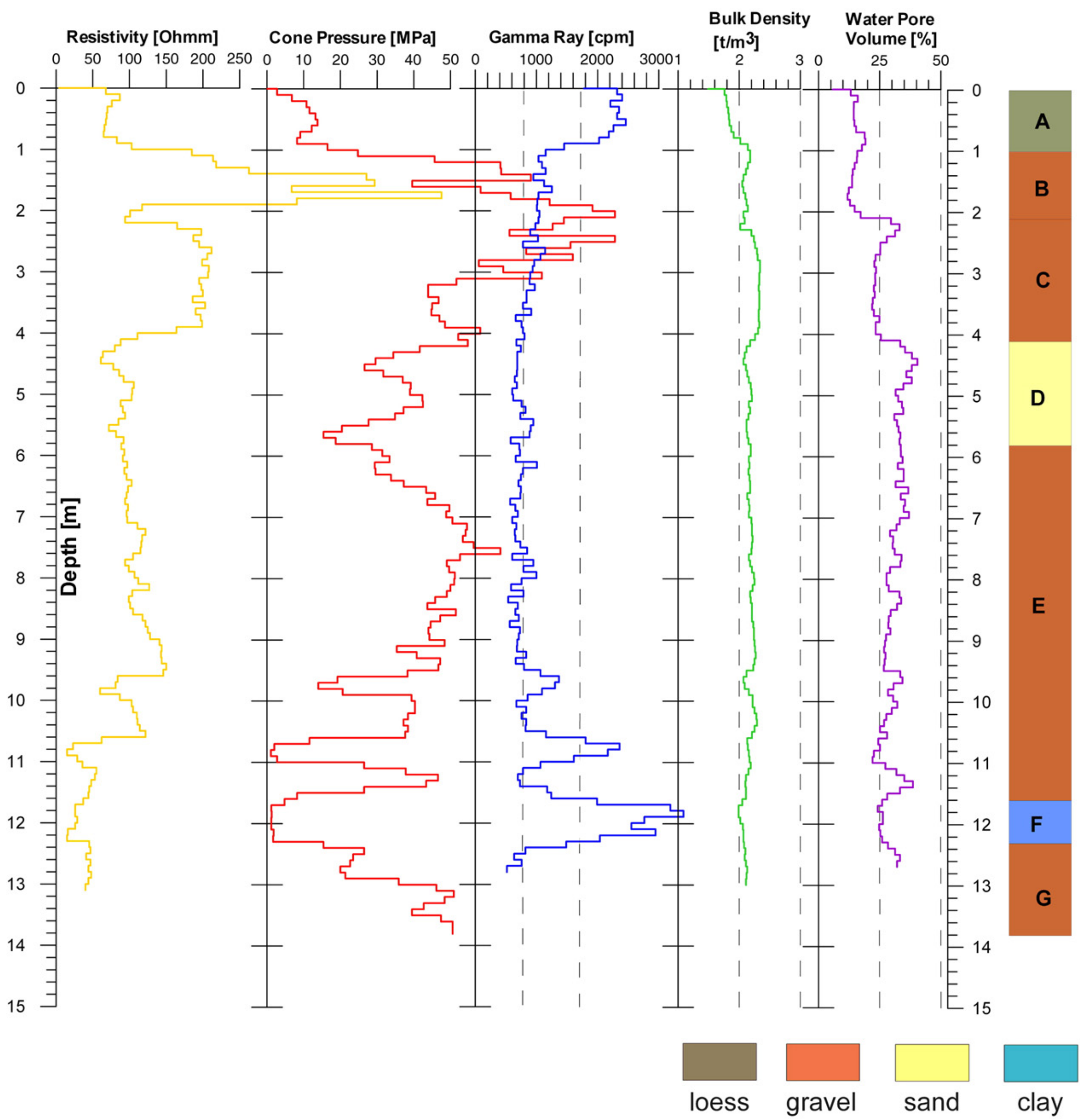

Fig. 8. CPTe logs and 1D geological interpretation on push point 103 from the profile K3.

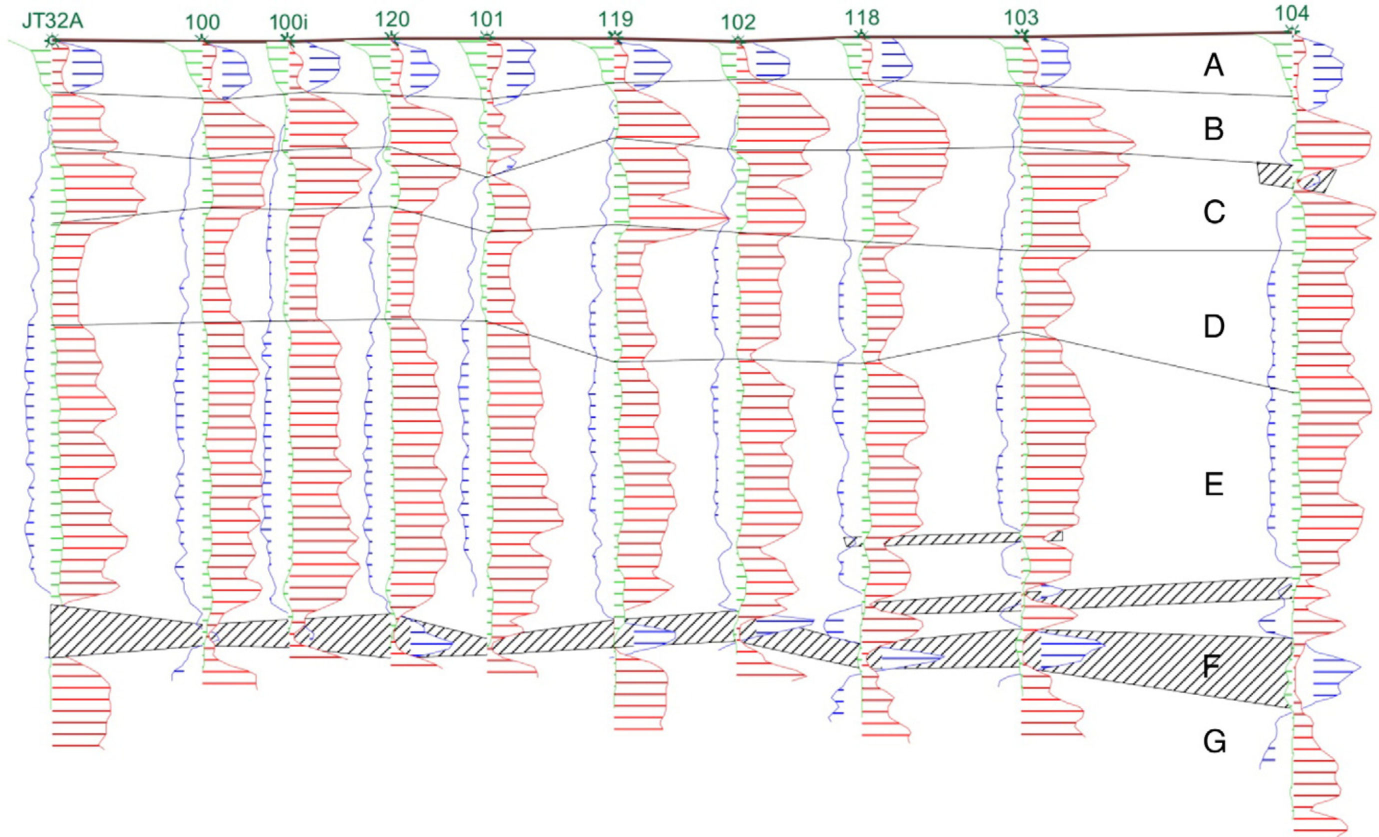

Fig. 9. CPTe logs and the 2D geological interpretation along the profile K3.

the hollow rods to register radiation data with a vertical spacing of also 10 cm (Fig. 6). Since the push hole stood stable down to the water table, after removing the measuring pipe, it was possible to measure the depth of the water table.

Two weeks after the CPTe tests a dense ERT measurement along the profile K3 was performed. The layout includes surface electrodes with 0.5 m spacing and borehole electrodes in boreholes 32, 31 and 62 with the separation of 0.5 m. In the inversion stage, the Occam's regularization (Constable et al., 1987), which results the smoothest model explaining the measured data was used. The resistivity section of the CPTe and the ERT measurements along the same profile K3 is shown in Fig. 7. A comparison of the two results gives an estimate of the resolution. The features of the first 6 meters below the surface are well resolved by the ERT method except for very small variations. On the other hand, remarkable is the lack of resolution between boreholes 32 and 31, where large discrepancy between the two methods can be observed that the ERT monitoring has less resolution than the CPTe data.

6. Data processing and geological interpretation

The processing of the raw data and geological interpretation was executed by the method of Fejes et al. (1997). The first step of data processing was the determination of the physical parameters for each CPT location using the appropriate calibration function. Then the cone resistance, the electrical resistivity where available, natural gamma activity, bulk density and water pore content logs were plotted versus depth. Afterwards geological sections were constructed and a geological interpretation in terms of separation into homogeneous layers was determined. Fig. 8 shows the CPT logs and the one dimensional geological model of seven layers, which are marked from top to bottom with letters from A to G. According to this model the following structure is sequenced: The top soil layer A and B are above the groundwater level. The material of layer B can be identified as gravel or debris. The uppermost aquifer is formed by layers C, D and E, which differ from each other by their various fractions of sand and gravel. Layer F is the aquifer base consisting of silt and clay series. The bottom layer G consists of sandy gravel. A more detailed description of the interpreted data including plots of all cross sections is provided by Tillmann et al. (2005).

To analyze the measurements in a qualitative way the CPT logs were gathered into cross sections. The CPT logs of cone pressure, natural gamma activity and bulk densities corresponded to the interpreted geological descriptions of the profile H3 are given in Fig. 9. Based upon the cross sections of the main three profiles, H3, K3 and K6, the detailed 3D geological model of the subsurface is constructed for the investigated area (Fig. 10).

7. Resistivity calculations

In order to obtain an accurate 3D resistivity model of the subsurface by the CPT data, first we need to determine the precise geological structure of the investigated area that is necessary to obtain confident input data for the delineation of the zones and the second, we need a reliable definition of the formation specific parameters which are used in resistivity calculations.

The De Witte model uses different formulas for the saturated and unsaturated zones therefore the delineation of these zones was performed after obtaining the detailed 3D geological model. This step was followed by the determination of the 3D distribution of the parameters by using the formulas (2) and (3). The porosity (Φ) and clay volumic fraction (V_{cl}) values were defined after the gamma-gamma and natural gamma logs of the CPT measurements. The resistivity of the pore water (R_w) was defined after analysis of water sampling in the monitoring wells. The water saturation (S_w) value was set to 0.8 and 0.5 in the two upper dry layers (A–B) and set to 1.0 downwards in the saturated zone. The clay resistivity (R_{cl}) was defined after in situ measurements and optimization processes. The

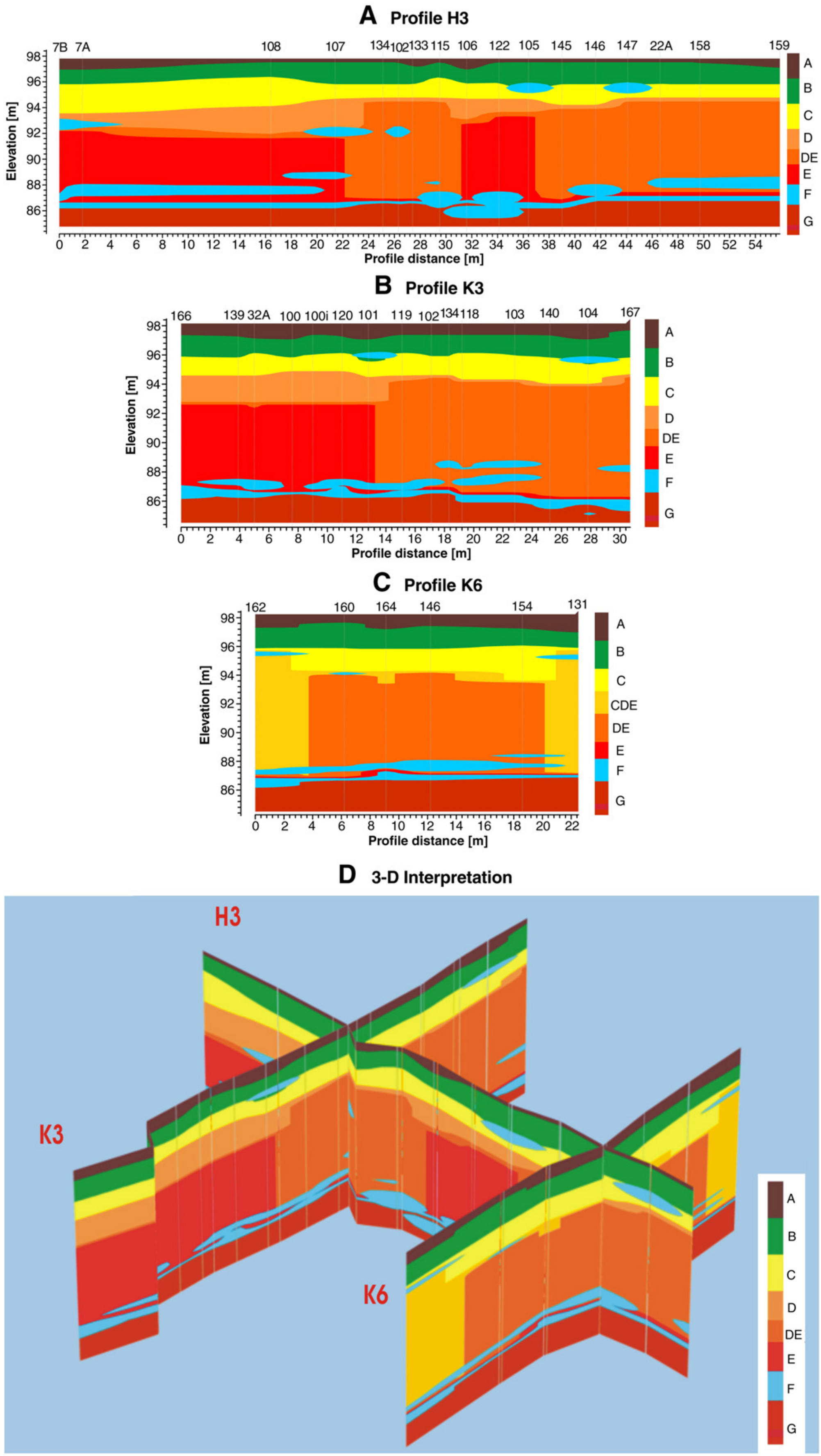

Fig. 10. A) Geological interpretation section of the profile H3. B) Geological interpretation section of the profile K3. C) Geological interpretation section of the profile K6. D) Result of 3D geological interpretation.

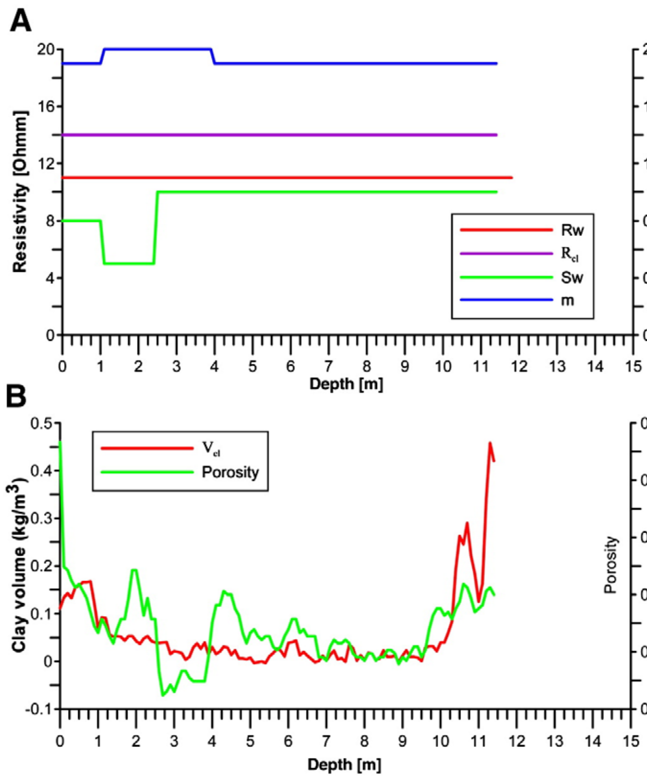

Fig. 11. A) Depth functions of the model parameters at push point 146. B) Plot of the clay volumic fraction and the porosity versus depth.

cementation factor or exponent (m) was set to 2 in layers B–C and it varies from 1.8 to 1.9 in the rest of the layers. Fig. 11 shows a good example for a result of the calculated depth functions of the empirical parameters from the push point 146. In the Fig. 11a, calculated parameters of the clay volumic fraction (V_{cl}), the pore water (R_w), the water saturation (S_w) and the cementation factor (m) are plotted versus depth, while the clay volumic fraction and the porosity changes are plotted versus depth in the Fig. 11b.

In order to analyse and prove our method's applicability, we tested it on a short section where measured resistivity data are available (profile R in the location map). Comparing the measured and calculated resistivity sections with the calculation of the deviation, significant differences appear mainly in the upper dry part where the location can be characterized by low clay content. Despite of these differences the comparison proved that the applied calculation method results suitable and reliable resistivity values (Fig. 12).

Consequently, 3D distribution of the electrical resistivity in the investigated depth range of 0–15 m is determined (Fig. 13). Comparing the resistivity and the geological sections a good correlation can be observed among the calculated resistivity distribution and the geological structure. The effect of the clay layer F and the thicker intermitting layers can be also marked clearly.

The simplified explanation of the subsurface geology corresponded to their resistivity values in the investigated test area of Krauthausen can be given as follows; A and B layers which are characterized by gravel or debris series are about 1–2 m depth and A has 10–30 Ω-m or 50–90 Ω-m resistivity values whereas B has 190–290 Ω-m resistivity values. The layer C is about 2 meters depth and it has the range of 110–180 Ω-m resistivity values. The mixture of the D-E series is about 7 m depth and they are in the range of 50–90 Ω-m or 110–170 Ω-m resistivity values. The C, D and E series form the uppermost aquifer which is characterized by sand and gravel. The layer F which is consisted of silt and clay series

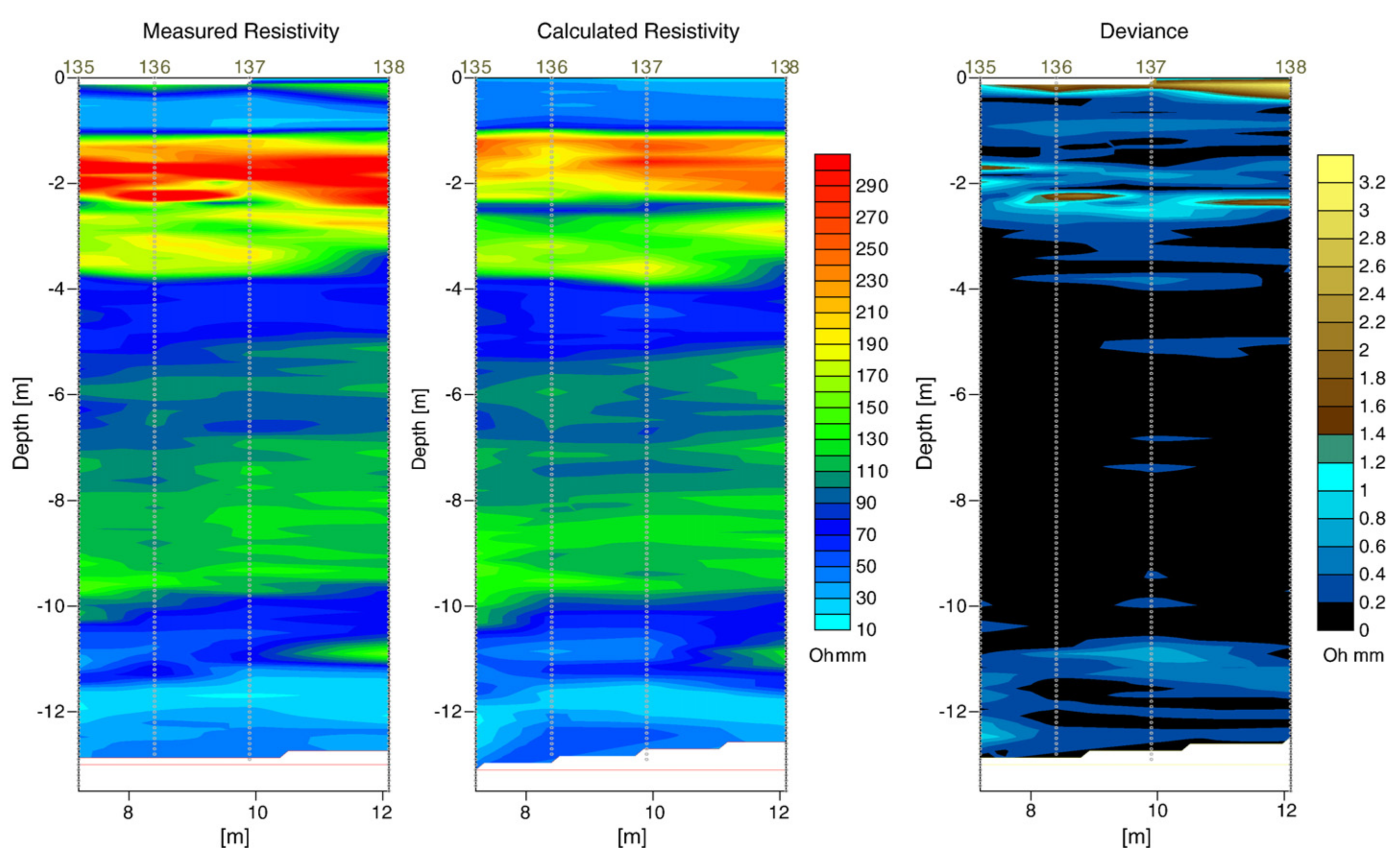

Fig. 12. Comparison of measured and calculated resistivity sections in the profile R.

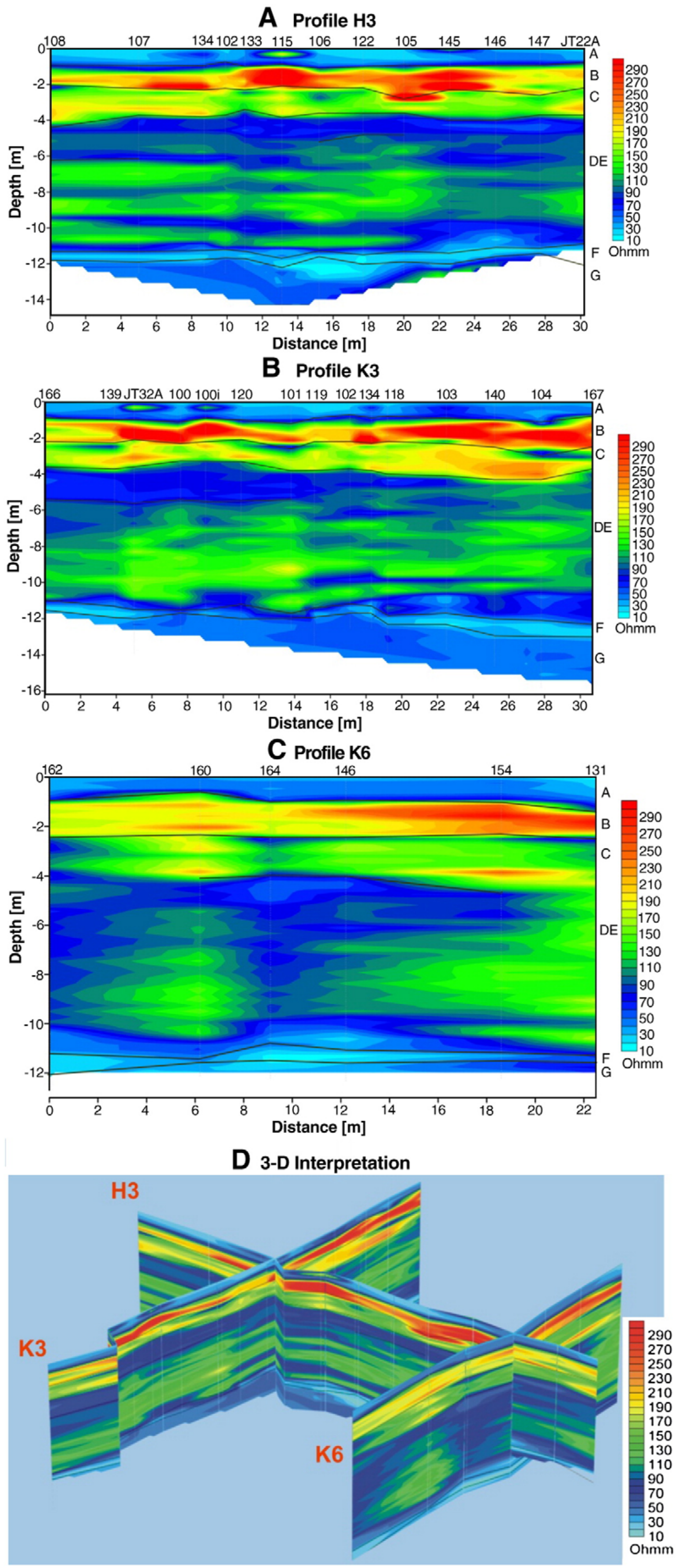

Fig. 13. A) Electrical resistivity section of the profile H3. B) Electrical resistivity section of the profile K3. C) Electrical resistivity section of the profile K6. D) Result of the 3D Electrical resistivity distribution calculated from CPT logs.

has 10–30 Ω-m resistivity values. The layer G which is characterized by sandy gravel series has the range of 50–80 Ω-m resistivity values.

8. Discussions and conclusions

The special version of a CPT(e) method is introduced as a promising tool for the investigating and modeling the fluid transport processes. The cone penetration technology is capable of resolving the structure of the test field in detail and logs the electric conductivity, density and water content during soil penetration. Various physical parameters can be recorded from dense CPT measurements such as the mechanical (cone resistance) and nuclear (natural gamma activity, gamma-gamma and neutron logs) parameters and these measurements are used in the resistivity calculations.

In order to determine a high-resolution resistivity distribution from the parameters of cone penetration tests, a promising and a reliable model is introduced. Using error calculations it is proved that De Witte model can handle the conductive effect caused by the clay content of the near surface sediments and on the river embankment area the application of the De Witte model is much more suitable than the Archie's method. The saturated zones and the depth zones for optimization processes were delineated after the reconstructed 3D geological model derived soil parameters of the CPT surveys.

The comparison between the densely recorded electrical resistivity data (CPTe-cone penetration test with electrical extension) and the ERT (electrical resistivity tomography) data showed us that there is a high resolution discrepancy between two methods due to the dense sampled CPTe data. Finally, the 3D electrical resistivity distribution of the test site of Krauthausen in Western Germany is mapped. The mapped 3D high-resolution spatial distribution of the electrical resistivity data on the test site can be used for future investigations such as calibration of ERT (electrical resistivity tomography) data measured during several tracer tests and other resistivity measurements, delineating the contamination problems of the investigated site and modeling the contamination and water transport processes with other various hydrogeological investigations.

Acknowledgements

This work is funded partly by the NATO Collaborative Linkage Grant No. 979868. This paper presents partly the results of research project GVOP-3.1.1-2004-05-0187/3.0 supported by the National Development Plan, the EU co-financed part of the Europe Plan. This work was supported by the Research Fund of Istanbul University, project number: UDP-4295/23092009. We would like to thank Klaus Holliger (Editor-in-Chief) and the reviewers for their constructive remarks.

References

Archie, G.E., 1942. The electrical resistivity log as an aid in determining some reservoir characteristics. Transactions of the American institute of Mining, Metallurgical and Petroluem Engineers 146, 54–67.

Constable, S.C., Parker, K.L., Constable, C.G., 1987. Occam's inversion: a practical algorithm for generating smooth models from EM sounding data. Geophysics 52, 289–300.

Daily, W., Ramirez, A., 1995. Electrical-resistance tomography during in-situ trichloroethylene remediation at the Savanna river site. Journal of Applied Geophysics 33, 239–249.

De Witte, A.J., 1957. Saturation and porosity from electric logs in shaly sands. Oil and Gas Journal 55 (9), 89.

Devarajan, S., Toumelin, E., Torres-Verdín, C., Thomas, E.C., 2006, Pore-scale analysis of the Waxman-Smits shaly sand conductivity model, SPWLA 47th Annual Logging Symposium, June 4-7, 2006.

Döring U., 1997, Transport der reaktiven Stoffe Eosin, Uranin und Lithium in einem heterogenen Grundwasserleiter, PhD thesis, Christian-Albrechts Universität Kiel, Kiel, Germany.

Englert, A., 2003. Measurement, Estimation and Modelling of Groundwater Flow Velocity at Krauthausen Test Site, PhD thesis. RWTH Aachen, Aachen, Germany.

Fejes, I., Jósa, E., 1990. The engineering geophysical sounding method: principles, instrumentation, and computerised interpretation. Geotechnical and Environmental Geophysics. Environmental and Groundwater, vol. II. SEG, Tulsa, Oklahoma, pp. 321–331.

Fejes, I., Szabadváry, L., Veró, L., Stickel, J., 1997. Geophysikalische Penetrationssondierungen, Methodenhandbuch Deponienuntergrund. Band Geophysik. Springer, Berlin, pp. 897–922.

Hördt, A., Blaschek, R., Kemna, A., Zisser, N., 2007. Hydraulic conductivity estimation from induced polarisation data at the field scale — the Krauthausen case history. Journal of Applied Geophysics 62, 33–46.

Kemna, A., Vanderborght, J., Kulessa, B., Vereecken, H., 2002. Imaging and characterisation of subsurface solute transport using electrical resistivity tomography (ERT) and equivalent transport models. Journal of Hydrology 267, 125–146.

LaBrecque, D.J., Yang, X., 2001. Difference inversion of ERT data: a fast inversion method for 3-D in situ monitoring. Journal of Environmental and Engineering Geophysics 6, 83–90.

Lambot, S., Binley, A., Slob, E., Hubbard, S., 2008. Ground penetrating radar in hydrogeophysics. Vadose Zone J. 7 (1), 137–139.

Li, W., Englert, A., Cirpka, O.A., Vereecken, H., 2008. Three-dimensional geostatistical inversion of flowmeter and pumping test data. Ground Water 46 (2), 193–201.

Lunne, T., Robertson, P.K., Powell, J.J.M., 1997. Cone penetration testing in geotechnical practice. Blackie Acad. and Prof., New York.

Nyari, Z., Kanlı, A.I., 2007. Imaging of buried 3D objects by using electrical profiling methods with GPR and 3D geoelectrical measurements. Journal of Geophysics and Engineering 4, 83–93.

Pidlisecky, A., Knight, R., Haber, E., 2006. Cone-based electrical resistivity tomography. Geophysics 71 (4), 157–167.

Singha, K., Gorelick, S.M., 2005. Saline tracer visualized with electrical resistivity tomography: field scale spatial moment analysis. Water Resources Research 41, W05023.

Slater, L., Binley, A., Versteeg, R., Cassiani, G., Birken, R., Sandberg, S., 2002. A 3D ERT study of solute transport in a large experimental tank. Journal of Applied Geophysics 49, 211–229.

Szücs, P., Madarasz, T., 2006. Complex hydrogeological modelling of multifunctional artificial recharge options of the Great-Forest Park in Debrecen, Hungary. In: Brebbia, C.A., Antunes do Carmo, J.S. (Eds.), Water Pollution VIII, Modelling, Monitoring and Management. WIT Press. ISBN: 1-84564-042-X, pp. 177–184.

Tillmann, A., Nyari, Z., Fejes, I., Englert, A., Vanderborght, J., Stickel, J., Bagi, J., Balazs, I., 2005, Cone Penetration Tests (CPT) on the Krauthausen Test Site Part I: Data Aquisition and Preliminary Interpretation of the Surveys 2003 and 2004, Project Report.

Tillmann, A., Eglert, A., Nyári, Zs., Fejes, I., Vanderborght, J., Vereecken, H., 2008. Characterization of subsoil heterogeneity, estimation of grain size distribution and hydraulic conductivity at the Krauthausen test site, using cone penetration test. Journal of Contaminant Hydrology 95, 57–75.

Vanderborght, J., Vereecken, H., 2002. Estimation of local scale dispersion from local breakthrough curves during a tracer test in a heterogeneous aquifer: the Lagrangian approach. J. Contam. Hydrol. 54, 141–171.

Vereecken, H., Döring, U., Hardelauf, H., Jaekel, U., Neuendorf, O., Schwarze, H., Seidemann, R., 1999. Analysis of solute transport in a heterogeneous aquifer: the Krauthausen Field experiment. 1. Experimental Set-up, Sediment Characterization and, Moment Analyses, Internal, Report No. 500798. Forschungszentrum Jülich, Jülich, Germany.

Vereecken, H., Döring, U., Hardelauf, H., Jaekel, U., Hashagen, U., Neuendorf, O., Schwarze, H., Seidemann, R., 2000. Analysis of solute transport in a heterogeneous aquifer: the Krauthausen field experiment. J. Contam. Hydrol. 45, 329–358.

Versteeg, R., Birken, R., Sandberg, S.K., Slater, L., 2000. Controlled imaging of fluid flow and a saline tracer using time lapse GPR and electrical resistivity tomography. Proceedings of the Symposium on the Application of Geophysics to Engineering and Environmental Problems 283–292.

Waxman, M.H., Smits, L.J.M., 1968. Electrical conduction in oil-bearing sands. Society of Petroleum Engineers Journal 8, 107–122.